Journal of the Taiwan Institute of Chemical Engineers 000 (2014) 1–6

Contents lists available at ScienceDirect

Journal of the Taiwan Institute of Chemical Engineers

journal homepage: www.elsevier.com/locate/jtice

Poly(vinylidene fluoride) membrane supported nano zero-valent iron for metronidazole removal: Influences of calcium and bicarbonate ions

Jiacheng Yang[a], Minping Zhu[a], Xiangyu Wang[a,*], Pedro J.J. Alvarez[b], Kunqian Liu[a]

[a] Faculty of Environmental Science and Engineering, Kunming University of Science and Technology, Kunming 650500, PR China
[b] Department of Civil and Environmental Engineering, Rice University, Houston, TX 77005, USA

ARTICLE INFO

Article history:
Received 3 July 2014
Revised 23 November 2014
Accepted 30 November 2014
Available online xxx

Keywords:
Metronidazole
Nano zero-valent iron
Calcium
Bicarbonate
Inorganic ions
Humic acid

ABSTRACT

This study examined the influences of calcium and bicarbonate ions on the performance of poly(vinylidene fluoride)-supported nano zero-valent iron (PSN) for metronidazole (MNZ) removal. The presence of Ca^{2+} and HCO_3^-, whether in their individual or collective forms with low or high levels, exerted differing degrees of inhibitions to MNZ removal by PSN, but these inhibitions were insignificant. Adding some other inorganic ions (*i.e.*, NH_4^+, SO_4^{2-}, Mg^{2+}, PO_4^{3-}, and NO_3^-) into MNZ solutions also caused suppressive effects and their inhibitive ability generally followed the order: $NH_4^+ > SO_4^{2-} > Mg^{2+} > PO_4^{3-} > NO_3^-$. Humic acid (HA) was found to introduce relatively larger inhibition to MNZ removal by PSN, whether in its single presence in MNZ solutions or in its coexistence forms with Ca^{2+} or HCO_3^- in MNZ solutions. The interaction of Ca^{2+}, HCO_3^- and HA with iron (oxy)hydroxides on PSN surface might contribute to these adverse impacts on PSN–MNZ reaction system. It was noteworthy that, even with 20 mg/L HA in MNZ solutions where high levels of Ca^{2+} and HCO_3^- were introduced, the MNZ removal by PSN was still above 73.37%. Results reported herein indicated the potential of using PSN to pretreat antibiotic wastewaters in complex environmental conditions.

1. Introduction

The past 15 years have witnessed a continuing interest in nano zero valent iron (NZVI) materials due to their high reactivity and cost-effectiveness in eliminating toxic pollutants from environment [1–3]. Recently, NZVI technology has also been used as a potential method to restore antibiotic-contaminated wastewaters [4,5]. Antibiotics, as emerging contaminants in environment, have antibacterial properties, toxicity, potential mutagenicity, and carcinogenicity, and thus pose a significant threat to the earth's ecosystems [6]. Therefore, it is of great necessity to remove them from various polluted sites [7].

Our previous work showed that poly(vinylidene fluoride) (PVDF) supported NZVI (PSN) hybrids demonstrated excellent performance for metronidazole (MNZ) removal from water *via* the reduction process induced by NZVI [8]. However, it was suggested that the reduction efficacy of NZVI-centered materials toward contaminants might be affected by stochastic geochemical constituents in aqueous matrix [9–13]. Bicarbonate ion, as a main substance in wastewater, was found to exert either positive or negative influences on the reduction reactivity of NZVI materials toward pollutants [9,10]. Differing impacts of Ca^{2+} on the removal of contaminants by zero-valent iron (ZVI)-based composites were also reported in previous work [9,11]. Meanwhile, special attention has been given to the combined effects of Ca^{2+} and HCO_3^- [11,12]. In addition, some other common cations (*e.g.*, Mg^{2+}, NH_4^+), anions (such as SO_4^{2-}, NO_3^- and PO_4^{3-}) and natural organic matters (NOMs) like humic acid (HA) were also found to introduce adverse effects on Fe^0 reactivity toward contaminants, depending on the physicochemical characteristics of NZVI composites and the types of the background species and pollutants [10,13].

Hence, evaluating the effects of various chemical constituents on the reduction reactivity of NZVI-centered materials toward antibiotics is of great importance in the viewpoint of environmental engineering. Unfortunately, to date, we lack such knowledge. Toward this end, efforts had been directed in this study to investigate how Ca^{2+} and HCO_3^- would influence the reduction efficacy of PSN toward MNZ in the presence of other common inorganic ions and HA.

2. Materials and methods

2.1. Materials

All chemicals were used as received without further treatment unless otherwise specified (refer to Table S1, in Supplementary material (SM)). The design principles for PSN hybrids were previously reported [8], and their synthetic procedures were provided in SM. Ultrapure water (resistivity > 18.25 MΩ cm) was used for preparation of all solutions. All cation and anion stock solutions were prepared using their

* Corresponding author. Tel.: +86 871 65170906; fax: +86 871 65170906.
E-mail address: wxya213@126.com, famdct@sohu.com (X. Wang).

http://dx.doi.org/10.1016/j.jtice.2014.11.033
1876-1070/

Table 1
Fitted parameters of two-parameter pseudo-first-order decay kinetics model for PSN–MNZ reaction system.

Run nos.	$CaCl_2$ (mM)	$NaHCO_3$ (mM)	Other inorganic solutes	Humic acid (mg/L)	$C_{ultimate}$ (mg/L)	k (1/min)	R^2
#001	0	0	5 mM NaCl	0	3.515	0.1015	0.9979
#002	0.4	0	5 mM NaCl	0	4.141	0.1003	0.9983
#003	2	0	5 mM NaCl	0	8.775	0.0962	0.9926
#004	0	2	5 mM NaCl	0	5.557	0.1036	0.9975
#005	0	8	5 mM NaCl	0	9.119	0.0881	0.9952
#006	0.4	2	5 mM NaCl	0	6.057	0.1049	0.9986
#007	0.4	8	5 mM NaCl	0	10.146	0.0880	0.9967
#008	2	2	5 mM NaCl	0	9.345	0.0985	0.9975
#009	2	8	5 mM NaCl	0	11.095	0.0881	0.9943
#010	2	0	5 mM NaCl + 10 mM NO_3^-	0	13.270	0.0648	0.9972
#011	2	0	5 mM NaCl + 10 mM SO_4^{2-}	0	9.856	0.0891	0.9932
#012	2	0	5 mM NaCl + 10 mM PO_4^{3-}	0	11.735	0.0773	0.9951
#013	2	0	5 mM NaCl + 10 mM NH_4^+	0	9.189	0.0952	0.9945
#014	2	0	5 mM NaCl + 10 mM Mg^{2+}	0	10.134	0.0883	0.9983
#015	0	8	5 mM NaCl + 10 mM NO_3^-	0	16.657	0.0527	0.9991
#016	0	8	5 mM NaCl + 10 mM SO_4^{2-}	0	9.376	0.0802	0.9971
#017	0	8	5 mM NaCl + 10 mM PO_4^{3-}	0	12.876	0.0730	0.9962
#018	0	8	5 mM NaCl + 10 mM NH_4^+	0	8.554	0.0940	0.9965
#019	0	8	5 mM NaCl + 10 mM Mg^{2+}	0	10.741	0.0807	0.9968
#020	0	0	5 mM NaCl + 10 mM NO_3^-	0	12.822	0.0769	0.9940
#021	0	0	5 mM NaCl + 10 mM SO_4^{2-}	0	8.889	0.0963	0.9934
#022	0	0	5 mM NaCl + 10 mM PO_4^{3-}	0	10.176	0.0842	0.9979
#023	0	0	5 mM NaCl + 10 mM NH_4^+	0	4.149	0.0985	0.9960
#024	0	0	5 mM NaCl + 10 mM Mg^{2+}	0	9.847	0.0926	0.9967
#025	0	0	5 mM NaCl	5	9.231	0.0905	0.9976
#025	0	0	5 mM NaCl	10	11.224	0.0801	0.9970
#027	0	0	5 mM NaCl	20	13.010	0.0682	0.9953
#028	2	0	5 mM NaCl	20	15.872	0.0552	0.9996
#029	0	8	5 mM NaCl	20	14.683	0.0619	0.9998
#030	2	8	5 mM NaCl	20	17.102	0.0456	0.9969

corresponding chloride and sodium salts, and the HA stock solution, which was stored in dark at 277 K, was prepared based on a method reported elsewhere [9].

2.2. Batch experiments

Batch experiments (see Table 1) were carried out in 60-mL sealed vials, each of which contained a piece of PSN hybrid (containing 9.52 ± 0.14 mg Fe^0) and 50 mL of 67.44 mg/L MNZ solution with differing combinations of Ca^{2+}, HCO_3^-, other inorganic ions and/or HA. 5 mM NaCl was used as the background electrolyte in solutions for all experiments [14]. The initial concentrations of Ca^{2+} were 0.4 mM and 2 mM, representing low and high hardness of waters, respectively, while those of HCO_3^- were 2 mM and 8 mM, respectively representing low and high alkalinity [12,14,15]. The concentrations of Mg^{2+}, NH_4^+, SO_4^{2-}, NO_3^- and PO_4^{3-} ions were all 10 mM, representing high levels of other common inorganic ions [16]. According to previous work [9], different levels of HA (5, 10 and 20 mg/L) were also designed to examine the impacts of NOM concentration on PSN–MNZ reaction system. Unless otherwise specified herein, all solution pHs were adjusted to 7.00 ± 0.10 by dropwise adding the solutions of 0.1 M HCl and 0.05 M NaOH, and determined using a PHS-2F precision pH meter (Shanghai, China). Then vials were sealed and mechanically shaken back and forth at 30 rpm in water bath shaker under room temperature. Solutions were sampled at pre-determined time intervals (up to 120 min) and filtered through 0.45 μm acetate cellulose membranes, followed by the residue analysis of MNZ. All batch experiments were run in duplicate under aerobic conditions.

2.3. Characterization and analysis

Surface morphologies of samples were observed using a high-solution field emission scanning electron microscope (FE-SEM, JEOL Ltd., Japan). Attenuated total reflectance-infrared (ATR-IR) spectra of fresh and aged PSN were examined by a Bruker Vertex 70 FT-IR spectrometer. Elemental information of PSNs before and after reaction was determined by X-ray photoelectron spectroscopy (XPS, PHI5000Versaprobe-II). The concentration of MNZ and loading of NZVI were determined by HPLC/MS (Agilent 1100) system and the 1,10-phenanthroline colorimetric method, respectively [8].

3. Results and discussion

In this study, it was found that, in all cases, the concentrations of MNZ in various solutions decreased fast within the first 40 min and later gradually flattened out (data not shown), which was consistent with our previous work [8]. Given such removal profiles, a two-parameter pseudo-first-order decay model was used to describe MNZ removal by PSN [8,17,18].

$$C_t = C_{ultimate} + (C_0 - C_{ultimate}) \times \exp(-kt) \quad (1)$$

where C_t is the concentration of MNZ (mg/L) at reaction time t, $C_{ultimate}$ represents the concentration of unreactive MNZ (mg/L) in solution, C_0 and k denote the initial concentration (mg/L) and reaction kinetics constant (1/min) of MNZ for each test, respectively. It was obvious that the removal of MNZ by PSN under differing conditions of Ca^{2+} and HCO_3^- could be well-described by such kinetics model with correlation coefficients (R^2) being above 0.99 (Table 1).

3.1. Influence of Ca^{2+} and HCO_3^-

Single additions of Ca^{2+} caused a marginal influence on MNZ removal by PSN. The drop of 5.22% in k at high concentration of Ca^{2+} might be the loss of reactive sites due to the formation of Ca–iron oxide complexes on PSN surface. The existence of Ca^{2+} within aged PSN was detected by the peaks at 345.8 and 349.2 eV (spectrum b, Fig. S4B), and strong peaks at 709.0–711.0 and 722.6–724.6 eV (spectra a and b, Fig. S4A), corresponding to $2p_{3/2}$ and $2p_{1/2}$ of Fe_2O_3, respectively [19,20], implied the oxidation of Fe^0 to Fe^{3+} during MNZ removal. The

Please cite this article as: J. Yang et al., Poly(vinylidene fluoride) membrane supported nano zero-valent iron for metronidazole removal: Influences of calcium and bicarbonate ions, Journal of the Taiwan Institute of Chemical Engineers (2014), http://dx.doi.org/10.1016/j.jtice.2014.11.033

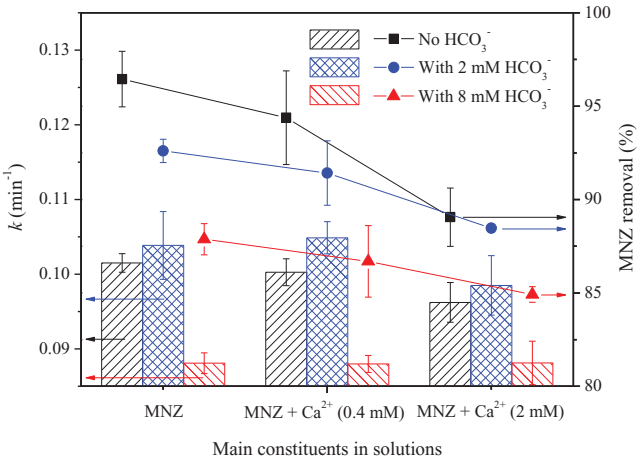

Fig. 1. Influence of varying levels of Ca^{2+} and HCO_3^- on PSN–MNZ reaction system under room temperature. Reaction conditions: 50 mL of 67.44 mg/L MNZ solution, pH 7.00, and reaction time 120 min. The errors bars, unless otherwise noted, indicate the standard deviations of duplicate experiments.

adsorbed Ca^{2+} would react with iron (oxy)hydroxides within PSN, partially covering surface reactive sites (Fig. S5b) and later resulting in the values of $C_{ultimate}$ being slightly elevated (see Table 1). Conversely, the PSN only reacted with MNZ exhibited more identifiable particle-shaped morphology (Fig. S5a). Note that the relatively small Fe^0 peaks at 706.2–707.2 and 718.4–718.6 eV [19,20], were also detected in Fig. S4A (spectra a and b), which might be a result of the protection of iron oxides [21]. This positive protection of PSN itself would contribute to the further removal of MNZ from water under complex conditions. Generally, the presence of Ca^{2+} coupling with iron oxides did not necessarily block the reactive sites of PSN or outcompete MNZ during the reaction process. When HCO_3^- was singly added into MNZ solutions, an interesting but antagonistic trend was observed: low HCO_3^- level slightly enhanced rate constant for MNZ removal over PSN, while the high one led to a decreased reaction rate constant compared to its absence (Fig. 1). The minor increase in k at low HCO_3^- level might be a result of both the buttering effect of HCO_3^- and the enhancement of Fe corrosion induced by its buttering effect [12,14,15]. On the other side, regardless of the promoted iron corrosion by the increased HCO_3^- level, its contribution to MNZ removal was not expected to be better than or as significant as that of its low level, because increasing concentration of HCO_3^- would improve the opportunities of HCO_3^- to react with amorphous iron (oxy)hydroxides [22,23], which might cover/block reactive sites (confirmed by FE-SEM image in Fig. S5c) and later exert negative impact on MNZ removal. The double peak at 1711.53 and 1640.52/cm (spectrum c, Fig. 2A) suggested the stretching of $–COO^-$ groups in HCO_3^- and the complexation of HCO_3^- with iron corrosion products. In addition, the peaks at 1550.02–1554.92/cm in spectra (a–h) were attributed to the binging of iron with $–COO^-$ groups of PAA within PSN [24].

Compared with MNZ solutions receiving 0.4 mM Ca^{2+}, a slight increase in k with slightly deceased removal rate of MNZ was observed when 2 mM HCO_3^- was added together with 0.4 mM Ca^{2+} (Fig. 1). This conflicting trend might be a result of the buffering impact of HCO_3^-. On one hand, HCO_3^- can accelerate Fe corrosion, which, in turn, provides more reactive species like H* in a short time for MNZ degradation, thus showing positive effect on MNZ reaction kinetics; however, on the other hand, HCO_3^- can react with the corrosion products or Ca^{2+} to form complicated complexes [14,15], which, undoubtedly, would become "nano/micro-barriers" to MNZ–PSN reaction system. Subsequent studies indicated that differing impacts of Ca^{2+} and HCO_3^- under changing levels existed. For instance, increasing concentration of HCO_3^- to 8 mM under low Ca^{2+} level would result in k being decreased by 13.33% with removal efficiency of MNZ decreased. The PSN reacted under high levels of Ca^{2+} and HCO_3^- was characterized by FE-SEM, XPS and ATR-IR techniques. The "mound-reef"-shaped surfaces unevenly encrusted with blocky colloids (Fig. S5d) implied the formation of surface complexes during MNZ removal. Such surface complexes were Ca^{2+}/iron oxides-centered, which were further confirmed by the peaks of Ca2p and Fe2p levels in spectrum c (Fig. S4). The disappearance of peak at 1711.53/cm in spectrum d (Fig. 2A) appeared to be ascribed to the reaction of Ca^{2+} with HCO_3^- on PSN surface [24], while the peak at 1639.40/cm was speculated to be indicative of combination of HCO_3^- with Ca^{2+} or iron corrosion products [14,15]. Considering the above discussion, it was assumed that the complexation of HCO_3^- with surface Fe corrosion hybrids of PSN and/or Ca^{2+} might be responsible for the reduction in MNZ removal.

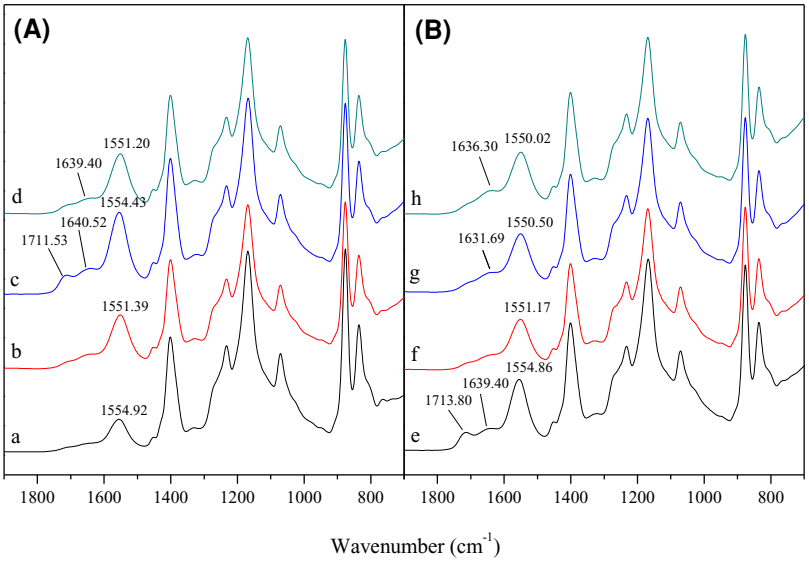

Fig. 2. ATR-IR spectra of spent PSN hybrids after reacting with MNZ solutions under differing levels of Ca^{2+} and HCO_3^- in the absence (A) or presence (B) of humic acid (HA) at room temperature: (a) no Ca^{2+} or HCO_3^-, (b) 2 mM Ca^{2+}, (c) 8 mM HCO_3^-, (d) 2 mM Ca^{2+} and 8 mM HCO_3^-, (e) 20 mg/L HA only, (f) 2 mM Ca^{2+} and 20 mg/L HA, (g) 8 mM HCO_3^- and 20 mg/L HA, and (h) 2 mM Ca^{2+}, 8 mM HCO_3^- and 20 mg/L HA. Other conditions: 50 mL of 67.44 mg/L MNZ solution, pH 7.00, and reaction time 120 min.

Please cite this article as: J. Yang et al., Poly(vinylidene fluoride) membrane supported nano zero-valent iron for metronidazole removal: Influences of calcium and bicarbonate ions, Journal of the Taiwan Institute of Chemical Engineers (2014), http://dx.doi.org/10.1016/j.jtice.2014.11.033

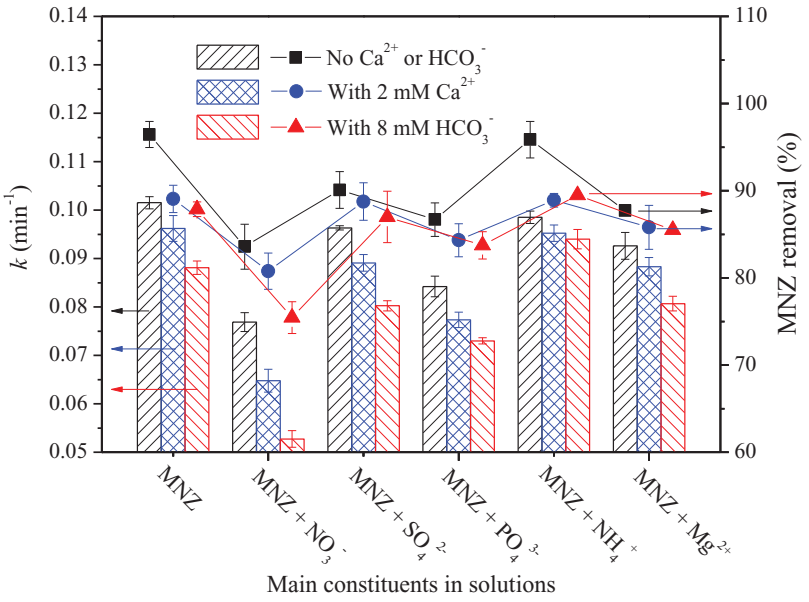

Fig. 3. Influence of Ca^{2+} and HCO_3^- on PSN–MNZ reaction system in the presence of other common inorganic ions under room temperature. Reaction conditions: 50 mL of 67.44 mg/L MNZ solution, pH 7.00, and reaction time 120 min. The concentrations of other anions and cations were all 10 mM.

3.2. Influence of Ca^{2+} and HCO_3^- in the presence of other inorganic ions

Evidently, whether Ca^{2+} and HCO_3^- existed or not, the additions of selected anions and cations introduced different extent of decrease in MNZ removal, and the decreased pseudo-first-order decay reaction kinetics constants of MNZ followed the order: $NH_4^+ > SO_4^{2-} > Mg^{2+} > PO_4^{3-} > NO_3^-$, ranging from 0.0952 to 0.0527/min, corresponding to the removal efficiencies ranging from 88.91 to 75.44% (Table 1 and Fig. 3). For NH_4^+, two possible factors can be assigned to explain its insignificant inhibition to MNZ removal by PSN: one is that NH_4^+ ions can continuously consume OH^- originated from Fe^0 corrosion process, thus retarding the formation of passive iron-based (oxy)hydroxides on PSN surface; the other is that NH_4^+ can restrain the formation of complexes of HCO_3^- with iron (oxy)hydroxides through its reaction with HCO_3^-. It is the two factors that make PSN provide the accessibility of reactive sites for MNZ degradation. By contrast, divalent Mg^{2+} caused greater adverse impacts on MNZ removal. This might be attributed to the formation of passivating surface layers as discussed above for Ca^{2+}. Compared to Ca^{2+}–HCO_3^- free case, the presence of NO_3^- in MNZ solutions caused rate constants being decreased by 24.27%, 36.22% and 48.07% for the cases of NO_3^-, Ca^{2+}–NO_3^- and HCO_3^-–NO_3^-, respectively (Fig. 3 and Table 1). The larger negative influence resulted from NO_3^- is understandable and self-evident due to its potential consumption of reactive species [25]. Note that, despite the sharply decreased k caused by NO_3^-, the lowest removal rate of MNZ is still above 75.44%, indicating that PSN can demonstrate comparatively ideal performance against MNZ removal under the condition of co-existing pollutants. The inhibition effects of SO_4^{2-} on MNZ removal were also observed (Fig. 3 and Table 1). As suggested in previous work [23], the adsorption and replacement of SO_4^{2-} with iron (oxy)hydroxides on the surface of PSN might contribute to the decline in MNZ removal. Clearly, the competition of single SO_4^{2-} ions for reactive sites and its adsorption on iron corrosion products was not strong enough to greatly decrease the reactivity of PSN except for the roles of Ca^{2+} and HCO_3^- themselves (Table 1 and Fig. 3). Nevertheless, the inhibition impacts were enhanced when PO_4^{3-} was added into MNZ solutions (Fig. 3). The strong affinity of PO_4^{3-} with iron (oxy)hydroxides together with Ca^{2+} and HCO_3^- as well as their complexation with iron corrosion products might result in such drops in MNZ removal efficiencies and kinetics [10,23]. Note that the decrease trend of MNZ removal caused by the selected inorganic ions at low levels of Ca^{2+} or HCO_3^- generally follows that of high levels (data not shown) , but the extent of decrease in MNZ removal is negligible other than the effects of inorganic ions themselves.

3.3. Influence of Ca^{2+} and HCO_3^- in the presence of HA

Fig. 4 depicts the impacts of Ca^{2+} and HCO_3^- on the removal of MNZ in the absence or presence of HA (20 mg/L) (the effects of HA concentrations on MNZ removal were also provided in Table 1 as a comparison). It is evidence that HA adversely influenced the removal of MNZ and the negative influence was reinforced with increased HA concentrations ranging from 5 to 20 mg/L (Table 1). The adverse impact might be a result of the adsorption of HA on PSN surface. To verify this speculation, FE-SEM and ATR-IR techniques were used to examine the reacted samples. Compared to PSN reacted in HA-free solutions (Fig. S5a), the PSN reacted in HA-containing solutions had a lager blocky surface with different levels of filling (Fig. S6a), which might result from the reaction of adsorbed HA with iron oxides within PSN [26]. This was further confirmed by ATR-IR spectrum e of Fig. 2B, in which two identifiable peaks at 1713.80 and 1639.40/cm, respectively, corresponding to the $–COO^-$ groups of HA and formation of Fe^{2+}/Fe^{3+}–humate complexes [14,27], existed.

Continuous decline in MNZ removal was detected as a result of the addition of high hardness (2 mM Ca^{2+}) into simulated solutions containing 20 mg/L HA. This might be associated with the decreased reactive sites for MNZ because of co-adsorption of Ca^{2+} and HA on PSN surface, and the co-adsorption of Ca^{2+} with HA was verified by the disappeared peaks at 1713.80 and 1639.40/cm (spectrum f, Fig. 2B) [14,28]. The adsorption of Ca^{2+} and HA on PSN surface, together with precipitation of Fe corrosion products, not only produced a decline in PSN reactivity (Fig. 4) but also a decrease in hydraulic conductivity and porosity (Fig. S6b displayed some blocked inner pores within PSN), which would finally lower the performance of PSN hybrids and their longevity. However, compared to solutions only receiving 8 mM HCO_3^-, the removal efficiency and k of MNZ deceased by 11.11% and 29.73%, respectively, when extra 20 mg/L HA were added, whereas those for the case of 2 mM Ca^{2+} reduced by 14.62% and 42.59%, respectively, under similar conditions (Table 1). Such trend might be

Please cite this article as: J. Yang et al., Poly(vinylidene fluoride) membrane supported nano zero-valent iron for metronidazole removal: Influences of calcium and bicarbonate ions, Journal of the Taiwan Institute of Chemical Engineers (2014), http://dx.doi.org/10.1016/j.jtice.2014.11.033

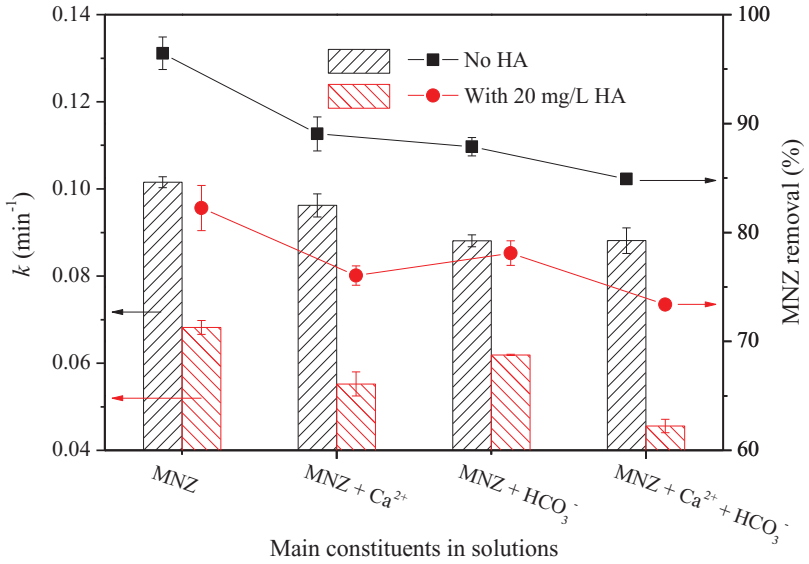

Fig. 4. Influence of Ca^{2+} or HCO_3^- on PSN–MNZ reaction system in the presence of HA under room temperature. Reaction conditions: 50 mL of 67.44 mg/L MNZ solution, pH 7.00, and reaction time 120 min. The concentrations of Ca^{2+} and HCO_3^- were 2 mM and 8 mM, respectively.

a result of the competition of HA for reactive sites and the buttering effect of HCO_3^-, which was different from the interaction of HA and Ca^{2+}. On one hand, HCO_3^- and HA with some negatively charged organic ligands can both reacted with Fe corrosion products [26,29], *i.e.*, the competition of HCO_3^- and HA existed; on the other hand, the co-presence of buttering effect of HCO_3^- and reducing action of HA could adjust or even reverse the electrostatic charges of PSN surfaces [12,14,26]. The overall role of two effects depending on the content of HA and HCO_3^- as well as other environmental parameters would finally control the performance of PSN during MNZ removal. Reacted PSNs were collected from MNZ solutions containing HA with sole HCO_3^-, and then were characterized using FE-SEM. Selected SEM image exhibited cauliflower- and block-like morphologies on the surface of aged PSN (Fig. S6c), which might stem from the formation of iron (oxy)hydroxycarbonate and iron–humate complexes. The appearance of peak at 1631.69/cm (Fig. 2B, spectrum g) further confirmed the existence of these iron–carboxyl complexes [12,14,26].

Notably, the removal efficiency and *k* of MNZ deceased to 73.37% and 0.0456/min, respectively, when its solutions containing 2 mM Ca^{2+} and 8 mM HCO_3^- received HA (20 mg/L). The steady and enhanced decline in MNZ removal under these conditions might originate in the formation of some passivated surface complexes (*e.g.*, iron oxide–humate complexes, carbonate green rust, $Ca(HCO_3)_2$ and their monodentate or multidentate complexes) [12,14,15], which would result in the blockage of surface reactive sites and pores and thus lead to inhibitory impacts. The irregular and noncrystal aggregates appeared in FE-SEM image (Fig. S6d) suggested the presence of the surface complexes. And the coexistence of iron oxide-centered hybrids within surface complexes was evidenced by peaks of XPS spectra at 710.0–711.0 and 722.8–724.6 eV (Fig. S4A, spectrum d) [19,20]. Meanwhile, weak small peaks at 706.8 and 719.0 eV were also detected, indicating the presence of Fe^0 within spent PSN surface due to the protection of surface iron oxides [30]. A peak at 1636.30/cm in ATR-IR spectrum h (Fig. 2B) verified the adsorption of HA and HCO_3^- centered compounds on PSN surface [10,12]. The variations in spectrum d for Ca2p level in comparison with spectra b and c (Fig. S4B) (*i.e.*, peaks at 349.4, 349.0, 347.8 and 346.8 eV in binding energy appeared and that at 349.2 eV disappeared) indicated the formation of calcium–humate/carbonate coupling with iron oxides over the whole reaction [12,14,15,22]. As a whole, the influences of HA with binary Ca^{2+} and HCO_3^- on efficacy of PSN toward MNZ were complex.

4. Conclusions

Generally, the Ca^{2+} and HCO_3^- with different concentrations and combinations did not materially affect the MNZ removal in spite of their detected unfavorable effects. The additions of selected inorganic ions resulted in the reaction kinetics constants of MNZ decreased with the order: $NH_4^+ > SO_4^{2-} > Mg^{2+} > PO_4^{3-} > NO_3^-$, ranging from 0.0952 to 0.0527/min, corresponding to the removal efficiencies ranging from 88.91 to 75.44%. HA, whether in its single form or combined forms with Ca^{2+} and/or HCO_3^-, introduced a larger inhibition to MNZ removal by PSN with its reaction kinetics constants reduced by 10.84–48.24%. Results reported herein suggest the attention to the roles of common geochemical factors in efficacy of NZVI-centered composites during their applications in environmental remediation.

Acknowledgments

This research was financially supported by National Natural Science Foundation of China (no. 51368025), Analytical & Testing Funding of Kunming University of Science and Technology (nos. 20130395 and 20130391), China Scholarship Council and Yunnan Training Programs of Innovation and Entrepreneurship for undergraduates (no. 10968063).

Supplementary materials

Supplementary material associated with this article can be found, in the online version, at doi:10.1016/j.jtice.2014.11.033.

References

[1] Bae S, Lee W. Influence of riboflavin on nanoscale zero-valent iron reactivity during the degradation of carbon tetrachloride. Environ Sci Technol 2014;48:2368–76.
[2] Němě Ek J, Lhotsky OE, Cajthaml T. Nanoscale zero-valent iron application for in situ reduction of hexavalent chromium and its effects on indigenous microorganism populations. Sci Total Environ 2014;485–486:739–47.
[3] Yu R, Chen H, Cheng W, Lin Y, Huang C. Monitoring of ORP, pH and DO in heterogeneous Fenton oxidation using nZVI as a catalyst for the treatment of azo-dye textile wastewater. J Taiwan Inst Chem Eng 2014;45:947–54.
[4] Chen J, Qiu X, Fang Z, Yang M, Pokeung T, Gu F, et al. Removal mechanism of antibiotic metronidazole from aquatic solutions by using nanoscale zero-valent iron particles. Chem Eng J 2012;181–182:113–19.

[5] Ghauch A, Tuqan A, Assi HA. Antibiotic removal from water: elimination of amoxicillin and ampicillin by microscale and nanoscale iron particles. Environ Pollut 2009;157:1626–35.
[6] González-Pleiter M, Gonzalo S, Rodea-Palomares I, Leganés F, Rosal R, Boltes K, et al. Toxicity of five antibiotics and their mixtures towards photosynthetic aquatic organisms: Implications for environmental risk assessment. Water Res 2013;47:2050–64.
[7] Kosma CI, Lambropoulou DA, Albanis TA. Investigation of PPCPs in wastewater treatment plants in Greece: occurrence, removal and environmental risk assessment. Sci Total Environ 2014;466–467:421–38.
[8] Yang J, Wang X, Zhu M, Liu H, Ma J. Investigation of PAA/PVDF–NZVI hybrids for metronidazole removal: synthesis, characterization, and reactivity characteristics. J Hazard Mater 2014;264:269–77.
[9] Lv X, Hu Y, Tang J, Sheng T, Jiang G, Xu X. Effects of co-existing ions and natural organic matter on removal of chromium (VI) from aqueous solution by nanoscale zero valent iron (nZVI)–Fe_3O_4 nanocomposites. Chem Eng J 2013;218:55–64.
[10] Tanboonchuy V, Grisdanurak N, Liao C. Background species effect on aqueous arsenic removal by nano zero-valent iron using fractional factorial design. J Hazard Mater 2012;205–206:40–6.
[11] Lai KCK, Lo IMC. Removal of chromium (VI) by acid-washed zero-valent iron under various groundwater geochemistry conditions. Environ Sci Technol 2008;42:1238–44.
[12] Mak MSH, Rao P, Lo IMC. Effects of hardness and alkalinity on the removal of arsenic(V) from humic acid-deficient and humic acid-rich groundwater by zero-valent iron. Water Res 2009;43:4296–304.
[13] Sun X, Wang X, Li J, Wang L. Degradation of nitrobenzene in groundwater by nanoscale zero-valent iron particles incorporated inside the channels of SBA-15 rods. J Taiwan Inst Chem Eng 2014;45:996–1000.
[14] Liu T, Rao P, Lo IMC. Influences of humic acid, bicarbonate and calcium on Cr(VI) reductive removal by zero-valent iron. Sci Total Environ 2009;407:3407–14.
[15] Lo IMC, Lam CSC, Lai KCK. Hardness and carbonate effects on the reactivity of zero-valent iron for Cr(VI) removal. Water Res 2006;40:595–605.
[16] Lim T, Zhu B. Effects of anions on the kinetics and reactivity of nanoscale Pd/Fe in trichlorobenzene dechlorination. Chemosphere 2008;73:1471–7.
[17] Lin K, Ding J, Huang X. Debromination of tetrabromobisphenol A by nanoscale zerovalent iron: kinetics, influencing factors, and pathways. Ind Eng Chem Res 2012;51:8378–85.
[18] Shu H, Chang M, Chen C, Chen P. Using resin supported nano zero-valent iron particles for decoloration of Acid Blue 113 azo dye solution. J Hazard Mater 2010;184:499–505.
[19] Yan W, Vasic R, Frenkel AI, Koel BE. Intraparticle reduction of arsenite (As(III)) by nanoscale zerovalent iron (nZVI) investigated with in situ X-ray absorption spectroscopy. Environ Sci Technol 2012;46:7018–26.
[20] Du Q, Zhang S, Pan B, Lv L, Zhang W, Zhang Q. Bifunctional resin–ZVI composites for effective removal of arsenite through simultaneous adsorption and oxidation. Water Res 2013;47:6064–74.
[21] Martin JE, Herzing AA, Yan W, Li X, Koel BE, Kiely CJ, et al. Determination of the oxide layer thickness in core−shell zerovalent iron nanoparticles. Langmuir 2008;24:4329–34.
[22] Jeen S, Gillham RW, Blowes DW. Effects of carbonate precipitates on long-term performance of granular iron for reductive dechlorination of TCE. Environ Sci Technol 2006;40:6432–7.
[23] Su C, Puls RW. Nitrate reduction by zerovalent iron: effects of formate, oxalate, citrate, chloride, sulfate, borate, and phosphate. Environ Sci Technol 2004;38:2715–20.
[24] Xiao S, Shen M, Guo R, Wang S, Shi X. Immobilization of zerovalent iron nanoparticles into electrospun polymer nanofibers: synthesis, characterization, and potential environmental applications. J Phys Chem C 2009;113:18062–8.
[25] Jiang Z, Lv L, Zhang W, Du Q, Pan B, Yang L, et al. Nitrate reduction using nanosized zero-valent iron supported by polystyrene resins: role of surface functional groups. Water Res 2011;45:2191–8.
[26] Xie L, Shang C. Role of humic acid and quinone model compounds in bromate reduction by zerovalent iron. Environ Sci Technol 2005;39:1092–100.
[27] Mak MSH, Rao P, Lo IMC. Zero-valent iron and iron oxide-coated sand as a combination for removal of co-present chromate and arsenate from groundwater with humic acid. Environ Pollut 2011;159:377–82.
[28] Dong H, Lo IMC. Influence of calcium ions on the colloidal stability of surface-modified nano zero-valent iron in the absence or presence of humic acid. Water Res 2013;47:2489–96.
[29] Giasuddin ABM, Kanel SR, Choi H. Adsorption of humic acid onto nanoscale zerovalent iron and its effect on arsenic removal. Environ Sci Technol 2007;41:2022–7.
[30] Yan W, Herzing AA, Li X, Kiely CJ, Zhang W. Structural evolution of Pd-doped nanoscale zero-valent iron (nZVI) in aqueous media and implications for particle aging and reactivity. Environ Sci Technol 2010;44:4288–94.

Please cite this article as: J. Yang et al., Poly(vinylidene fluoride) membrane supported nano zero-valent iron for metronidazole removal: Influences of calcium and bicarbonate ions, Journal of the Taiwan Institute of Chemical Engineers (2014), http://dx.doi.org/10.1016/j.jtice.2014.11.033